J Mater Sci (2007) 42:1477–1482
DOI 10.1007/s10853-006-0977-8

DSC and TEM analysis of lattice defects governing the mechanical properties of an ECAP-processed magnesium alloy

B. Mingler · O. B. Kulyasova · R. K. Islamgaliev · G. Korb · H. P. Karnthaler · M. J. Zehetbauer

Received: 28 June 2006 / Accepted: 19 September 2006 / Published online: 4 January 2007
© Springer Science+Business Media, LLC 2006

Abstract The mechanical properties of the Mg alloy AM60 can be improved significantly by severe plastic deformation (SPD). The lower the temperature (down to 150 °C) of equal channel angular pressing (ECAP) the higher is the resulting strength (up to 310 MPa) which can be ascribed to the concomitant decrease of grain size (down to 1 μm). After ECAP-processing at temperatures 150–210 °C the ductility remains at about the same high level (~15%) as in the initial material. This is explained with the presence of $Al_{12}Mg_{17}$ precipitates with a size of about 500 nm, which decrease the remaining concentration of Al in the solid solution of the matrix. Differential scanning calorimetry (DSC) revealed four peaks during heating runs. The most remarkable peak occurs at 390 °C in the initial sample, and at 360 °C in the material ECAPed at 150 °C. Transmission electron microscopy (TEM) analyses showed that this peak can be associated with the dissolution of the $Al_{12}Mg_{17}$ precipitates as well as with the annealing of dislocations and possibly vacancy clusters, and that ECAP has the potential to induce a shift of a phase boundary to lower temperatures because of ECAP induced lattice defects.

B. Mingler (✉) · H. P. Karnthaler · M. J. Zehetbauer
Institute of Materials Physics, University of Vienna,
Boltzmanngasse 5, Vienna A-1090, Austria
e-mail: bernhard.mingler@univie.ac.at

O. B. Kulyasova · R. K. Islamgaliev
Institute of Physics of Advanced Materials,
Ufa State Aviation Technical University,
K.Marks 12, Ufa 450000, Russia

G. Korb
Austrian Research Center Seibersdorf GmbH,
Seibersdorf, Austria

Introduction

Lightweight magnesium alloys offer high specific strengths. Therefore they are mainly used for structural applications in the automotive and aerospace industry [1–9]. Currently the most common Mg alloys contain Al and in addition Zn or Mn (AZ and AM series, respectively). Because of the low formability of these Mg alloys their components are generally fabricated by casting methods leading to yield strength and ductility values less than 250 MPa and 10%, respectively. An improvement of the mechanical properties of metals and alloys can be achieved by grain refinement. In many different metals the process of equal channel angular pressing (ECAP) has been successfully applied for such a refinement [10–16]. Recently, it was shown for the Mg alloy AM60 that, with appropriate selection of the ECAP temperature, both a high strength and a considerable ductility can be achieved [17]. It was the aim of the present work to study the presence and arrangement of lattice defects in the ECAPed Mg alloy AM60 as a function of annealing temperature with calorimetric and transmission electron microscopy (TEM) methods.

Experimental

Cast billets of the magnesium alloy AM60 (Mg–6%Al–0.13%Mn) were subjected to an ECAP tool with two

channels (circular in cross-section) intersecting at an angle of 120°. The processing route B_C was used by which the samples were rotated by 90° in the same direction between two consecutive passes. The initial rods, having a diameter of 20 mm and a length of 100 mm, were pressed through the ECAP tool 10 times. To study the influence of the ECAP temperature on the mechanical properties and the microstructure, three sets of samples were pressed at the temperatures 150, 210 and 350 °C.

Small tensile specimens with a gage length of 4 mm and a cross section of 1.0×0.4 mm^2 were prepared. In case of ECAPed samples, they were machined from platelets cut normal to the pressing axis. The variation of stress with strain was recorded at room temperature (RT) using a computer-controlled tensile testing machine described elsewhere [18]. The strain rate used in tensile tests was 1×10^{-3} s^{-1}. For each tensile curve three single tests were averaged (maximum deviation: 1% in strain, 10 MPa in stress).

Calorimetric measurements were performed using a differential scanning calorimeter (Perkin Elmer DSC 7) connected to a PC and a thermal analysis instrument controller (Perkin Elmer TAC 7/DX). Thermal scans were carried out in the range 20–500 °C at a heating rate of 30 K/min under flowing Ar. Specimens for calorimetric measurements with 6 mm in diameter were cut from ECAPed samples (plane normal to the pressing axis) using a spark-erosion machine. Then they were ground to a final mass of about 43 mg. To study the effects of thermal treatments with TEM, DSC heating runs were stopped at different temperatures (100, 230, 330 and 400 °C) from which the samples were quenched by 200 K/min in order to freeze the microstructure.

The structural changes associated with ECAP pressing at different temperatures and additional thermal treatments were investigated using a Philips CM200 TEM equipped with an energy-dispersive X-ray spectrometer (EDS). For the preparation of the TEM foils, discs having a diameter of 2.3 mm were punched from slices of the ECAPed samples. Then they were ground to a thickness of ~0.15 mm and finally electropolished to perforation using a twin-jet electro-polishing facility with a mixture of 1% perchloric acid and 99% ethanol.

Results

Tensile tests

Figure 1 displays the tensile properties of the initial cast alloy as well as of the ECAPed samples processed at three different temperatures (150, 210 and 350 °C). The lower the ECAP temperature the higher is the strength level observed. After ECAP at 150 °C the AM60 alloy exhibits the highest ultimate tensile strength (310 MPa) but retains the high ductility (15%) of the undeformed cast alloy.

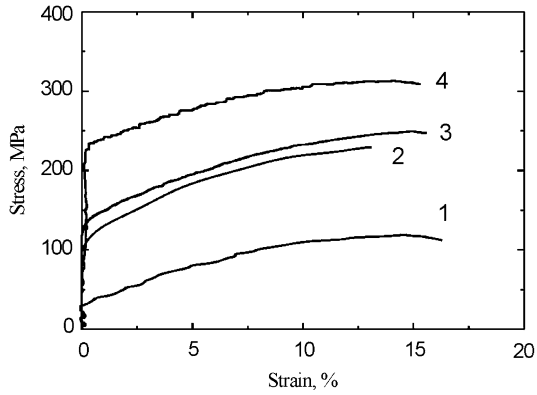

Fig. 1 The variation of engineering stress with engineering strain for the AM60 alloy processed by ECAP at different temperatures: (1) initial cast alloy, (2) 350 °C, (3) 210 °C, (4) 150 °C; with average grain sizes (1) 50 μm, (2) 5 μm, (3) 2 μm, (4) 1 μm

Differential scanning calorimetry (DSC)

DSC curves of the initial (undeformed) sample and of samples ECAPed at three different temperatures (150, 210 and 350 °C) are shown in Fig. 2; data are specified in detail in Table 1.

In all curves of the ECAPed samples four peaks can be identified. The first peak is located at a temperature of about 150 °C. The second peak at about 300 °C is absent in the case of the initial as-cast alloy, whereas all the ECAPed samples show this peak. Peak 3 occurs at 390 °C in the case of the initial alloy and is shifted to lower temperatures (from 385 to 360 °C) with decreasing ECAP temperature. This shift of peak 3 (p3 → p3-ECAP) is illustrated in a schematic sketch of a part of the phase diagram (Fig. 3). Peak 4 appears at the same temperature (about 430 °C) in case of all samples and is not included in Table 1.

Transmission electron microscopy (TEM)

Figure 4 shows the characteristic microstructures observed in the AM60 alloy subjected to ECAP at different temperatures. ECAP at a temperature of 350 °C leads to a rather heterogeneous microstructure. Equiaxed grains with a size of 5–10 μm were observed in 60–70% of the area investigated. The area left is occupied by elongated grains with a width of 0.2–1.5 μm and a length of 5–15 μm (Fig. 4a); an accurate

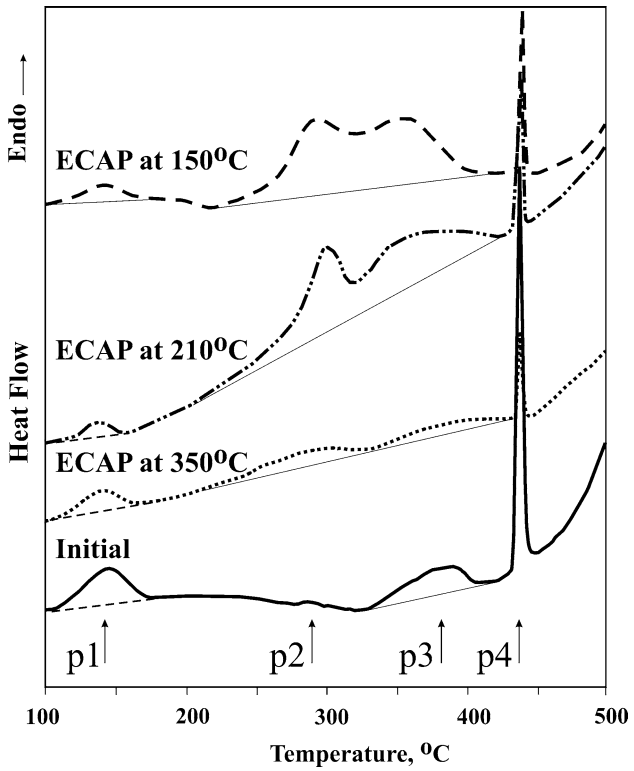

Fig. 2 DSC curves as recorded from the initial sample and from samples being ECAPed at the temperatures given

Table 1 Data of the first three DSC peaks in Fig. 2

Condition	Peak 1		Peak 2		Peak 3	
	T_p [°C]	ΔH [J/g]	T_p [°C]	ΔH [J/g]	T_p [°C]	ΔH [J/g]
Initial	149	0.7	–	–	390	0.8
ECAP at 350 °C	148	0.4	285	0.7	385	0.4
ECAP at 210 °C	147	0.2	310	2.3	370	1.8
ECAP at 150 °C	144	0.4	295	2.6	360	2.3

ΔH, heat of phase transformation; Tp, peak temperature

analysis revealed that some of them are twins. Finely dispersed small particles with an average diameter of ~30 nm were observed in the grain interiors.

A more uniform microstructure consisting of equiaxed grains with a mean grain size of ~2 μm was observed in the ECAPed samples processed at a temperature of 210 °C (Fig. 4b). Two different types of precipitates could be distinguished in these specimens (Fig. 5a). The first type is similar to the finely dispersed small particles observed in the samples ECAPed at 350 °C having the same size of about 30 nm (marked by arrows in Fig. 5a). Precipitates of a second type have been found in high density, which exhibited an average diameter of about 0.5 μm (Fig. 4b); they are inhomogeneously distributed and

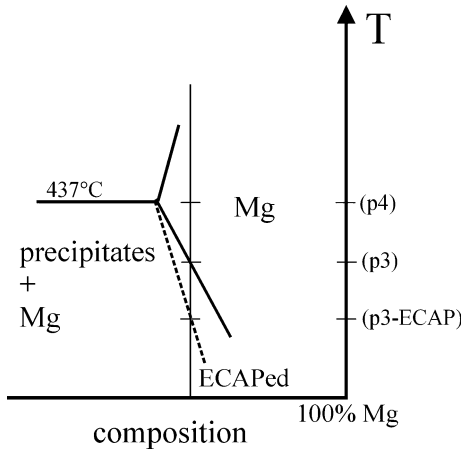

Fig. 3 Schematic sketch of a part of the phase diagram of the AM60 alloy. The vertical line represents the composition of the AM60 alloy

often form larger clusters both in the grain interiors and in the grain boundaries.

The microstructure of the samples processed by ECAP at a temperature of 150 °C is rather uniform with a mean grain size of about 1 μm (Fig. 4c). In these specimens also two types of precipitates with different size were observed, but in contrast to the samples ECAPed at 210 °C, the larger precipitates are distributed more homogeneously.

In all samples (after ECAP at different temperatures) a high dislocation density was observed (only visible under special image conditions). An EDS analysis demonstrated the differences concerning the chemical composition of the two types of precipitates (Fig. 5b). It clearly showed that the large particles consist of Mg and Al. According to the Mg-Al phase diagram it should be the γ-$Al_{12}Mg_{17}$ phase [19]. The small precipitates contain Mn with the probable composition Al_6Mn (Fig. 5b). These small particles have been equally found in all samples regardless of mechanical and thermal treatment. Mn is mainly added to improve the corrosion resistance of the alloy.

For reliable interpretation of the DSC results, TEM images of the ECAP samples processed at 150 °C were taken after linear heating to different temperatures (100, 230, 330 and 400°C) which lie in between the DSC peaks (Fig. 6), and subsequently quenched to RT. The microstructure after annealing at 230 °C (corresponding to a temperature between peak 1 and 2) is very similar to that after annealing at 100 °C, previous to peak 1 (compare Fig. 6a with Fig. 6b). The grain size and the precipitate density remain unchanged indicating that dissolution of precipitates does not take place at these temperatures. Annealing at a temperature beyond the second peak (330 °C, Fig. 6c) results in

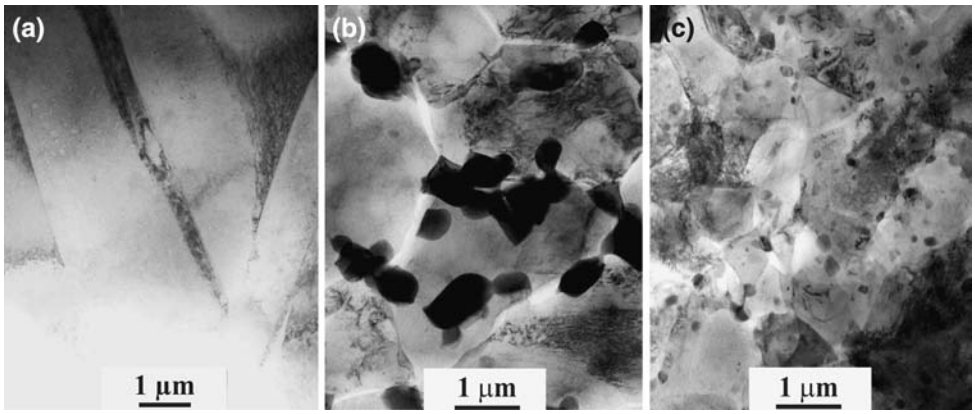

Fig. 4 Microstructures of the Mg alloy AM60 after ECAP processing at different temperatures (**a**) 350 °C, (**b**) 210 °C, (**c**) 150 °C

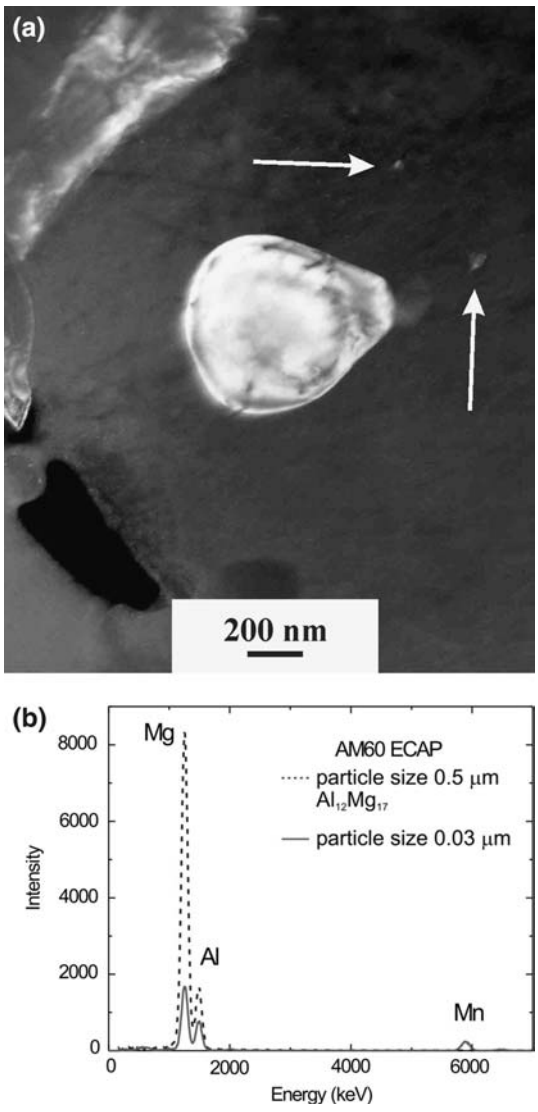

Fig. 5 (**a**) Dark field image of two different types of precipitates (the small ones are marked by arrows), (**b**) EDS spectrum of the two types of precipitates

some grain growth (up to 4 μm) and in some decrease of dislocation density. Precipitates of both types were observed. However, after annealing at 400 °C (temperature after peak 3) the grain structure shows up recrystallization (Fig. 6d). The average grain size is about 5 μm and neither dislocations nor precipitates of the second type (the large ones) were observed (it is interesting to note that fine dispersed particles of the first type are still present).

Discussion

The tensile tests showed that 10 ECAP passes carried out at temperatures between 150 °C and 210 °C result in a combination of high strength with considerable ductility. This SPD deformation procedure induces a rather uniform microstructure, which consists of small grains (between 1 and 2 μm); in addition, two types of precipitates were observed which are distributed more or less homogeneously across the sample (see Fig. 4c). Since the small particles have been equally found in all samples regardless of mechanical and thermal treatment they do not seem to be responsible for the changes of mechanical properties observed. According to the formation enthalpies of the large precipitates shown up in Table 1, their volume fraction varies by a factor 1.3 which also seems to small to account for the differences in strength between the samples ECAPed at 150 and 210 °C. Thus it is supposed that the enhancement of strength in the ECAPed samples (cf. Fig. 1) is correlated with the grain refinement depending on the ECAP temperature applied: the highest ultimate tensile strength was measured in the sample processed at 150 °C containing the smallest grains, with a size of about 1 μm. With increasing ECAP temperatures (210 and 350 °C) the grain size increases to 2

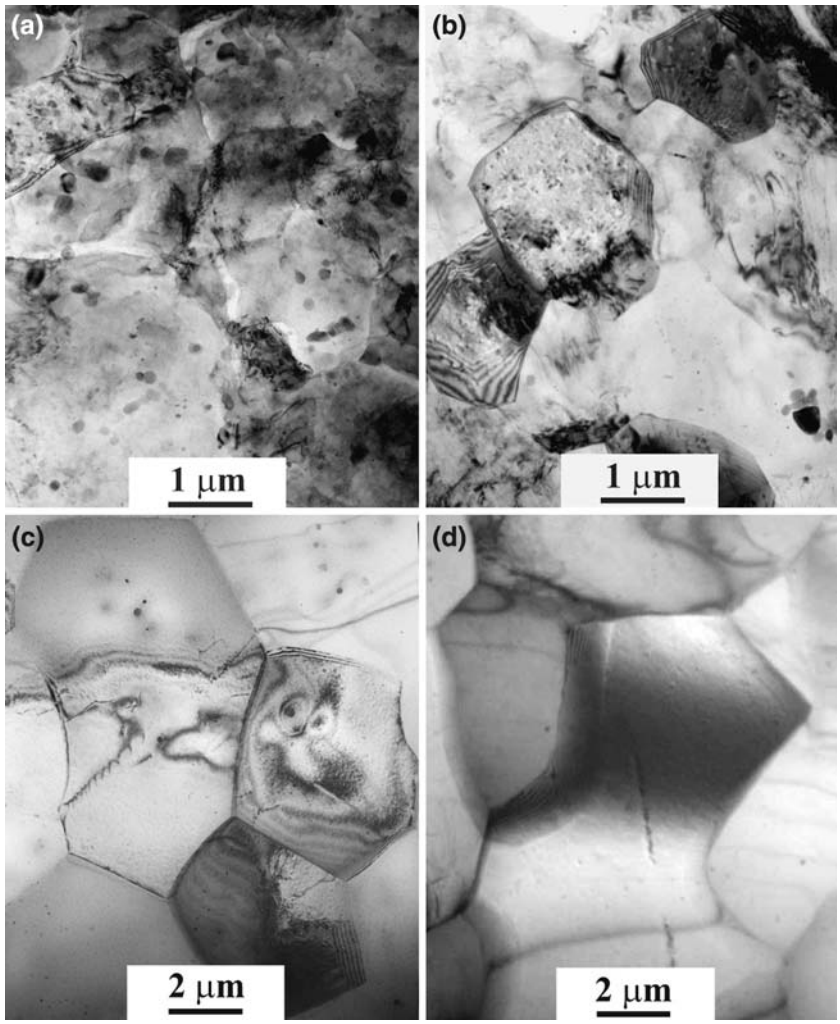

Fig. 6 The evolution of the microstructure after ECAP (processed at 150 °C) and linear heating up to different temperatures: (**a**) 100 °C, (**b**) 230 °C, (**c**) 330 °C, (**d**) 400 °C

and 5 μm, respectively, and the corresponding strength decreases. For the high ductility of the samples ECAPed at 150 and 210 °C, two explanations are considered: (1) the ductility increases due to the decreasing amount of solute atoms which are consumed by the formation of the large precipitates; this explanation is suggested by the fact that the alloys ECAPed at 150 and 210 °C exhibit a higher ductility than that ECAPed at 350 °C where (according to the TEM findings) these large precipitates are absent; (2) the ductility increases with decreasing grain size since small grain sizes (at least of the order of a few μm) enable grain boundary sliding [20]. We prefer the first explanation because the second one does not combine with our measurements (cf. Fig. 1) where the sample with the smallest grain size (1 μm) ECAPed at 150 °C does not exhibit any increase of ductility in comparison with the sample with grain size (2 μm) ECAPed at 210 °C.

Annealing at a temperature of 100 °C after ECAP (processed at 150 °C) seems to have only small influence on the microstructure (compare Fig. 4c with Fig. 6a). Even the annealing at a higher temperature (230 °C) leads to a rather unchanged microstructure (cf. Fig. 6b). Moreover, the first peak of DSC analysis also occurs with the initial state of the material; all these three observations lead us to the assumption that this peak results from the annealing of vacancies, which stem from either quenching or the ECAP deformation [21] and which does not change significantly the microstructure.

The reason for the appearance of the second peak in DSC at 295°C is supposed to be connected with some dislocation mobilization. This is confirmed by the fact that this peak does not occur in the initial state. However, inspection by TEM did not show up a marked dislocation annealing until 330 °C. Therefore it is assumed that the second peak in calorimetry represents mainly some rearrangement of ECAP induced dislocations.

After annealing at 400 °C no large precipitates ($Mg_{17}Al_{12}$) of the second type are visible; moreover,

the grain size is clearly larger than after annealing at 330 °C, and no free dislocations can be seen. Therefore it is supposed that, besides the annealing of dislocations, the third peak essentially reflects the dissolution of these precipitates and the redistribution of Al in the Mg matrix. This assumption is confirmed by the fact that the third peak also occurs in the DSC of the initial alloy, and the same interpretation has been given by Bassani et al. [22] in a combined study by calorimetry and SEM. It is important to note that in the initial alloy the third peak arises at a rather high temperature (390 °C) and in the ECAPed samples the peak is shifted to lower temperatures with decreasing ECAP temperature (from 385 to 360 °C) (see Fig. 3). This is a strong indication that the process of ECAP deformation has a marked influence on the precipitation kinetics. Because of the fact that the deformation induced vacancies have already annealed through peak 1, it is believed that the enhancement of precipitation dissolution is mainly caused by the ECAP induced dislocations and other defects which are still present at temperatures below the annealing temperature of this peak, and which will anneal at the occasion of particle dissolution. The observations by TEM (Fig. 6d) exhibited a strongly recrystallized structure being present at $T = 400$ °C which favours the ECAP induced dislocations to be important here; however, the annealing of vacancy clusters cannot be excluded [21, 23].

Similarly to the conclusions of Bassani et al. [22], the fourth peak is considered to be the melting peak at which the solid solubility limit of Al (about 12 wt.%) is exceeded and where the dissolution of the small Al containing precipitates starts (compare Fig. 2).

Conclusions

ECAP of the Mg alloy AM60 leads to enhanced mechanical properties. 10 ECAP passes processed at 150 °C result in an ultimate tensile strength of 310 MPa and in a ductility as high as 15% similar to that measured in the undeformed material. These excellent mechanical properties are the consequence of a small grain size (~1 μm) and the presence of $Al_{12}Mg_{17}$ precipitates with a size of about 500 nm, which decrease the remaining concentration of Al in the solid solution of the matrix. An increase of the ECAP temperature (210 and 350 °C) yields a decrease of the strength due to the increase in grain size, while the concomitant decrease in ductility can be related to the increase of concentration of Al in the matrix. TEM analysis revealed that the third peak observed in DSC is associated with the dissolution of the $Al_{12}Mg_{17}$ precipitates, and the annealing of ECAP induced dislocations. This peak occurs at 390 °C in the case of the undeformed material, and is shifted to lower temperatures in the case of the ECAPed materials. This shift of a phase boundary to lower temperatures can be explained by the presence of ECAP induced dislocations and maybe of vacancy clusters.

Acknowledgements Financial support by the INTAS YS project # 3489, the Austrian FWF (project P17095-N02) and the Russian program ''Development of the Higher School Scientific Potential'' is gratefully acknowledged.

References

1. Kumar S (2006) J Mat Eng Perf 15:41
2. Cole GS (2003) Mater Sci Forum 43:419–422
3. Froes FH (1994) Mater Sci Eng A 184:119
4. Taub AI (2006) MRS Bulletin 31:336
5. Rosen GI, Segal G, Lubinsky A (2005) Mater Sci Forum 509:488–489
6. Kaneko T, Suzuki M (2003) Mater Sci Forum 67:419–422
7. Blawert C, Hort N, Kainer KU (2004) Transactions Ind Inst Met 57:397
8. Furuya H, Matunaga S, Kogizo N (2003) Mater Sci Forum 261:419–422
9. Luo A, Renaud J, Nakatsugawa I, Plourde J (1995) JOM 47:28
10. Valiev RZ, Islamgaliev RK, Alexandrov IV (2000) Prog Mater Sci 45:103
11. Iwahashi Y, Horita Z, Nemoto M, Langdon TG (1998) Acta mater 46:3317
12. Mingler B, Karnthaler HP, Zehetbauer M, Valiev RZ (2001) Mater Sci Eng A 319–321:242
13. Furukawa M, Horita Z, Nemoto M, Langdon TG (2001) J Mater Sci 36:2835
14. Kim WJ, An CW, Kim YS, Hong SI (2002) Scripta mater 47:39
15. Valiev RZ, Langdon TG (2006) Progr Mater Sci 51:881
16. Mingler B, Stolyarov VV, Zehetbauer M, Lacom W, Karnthaler HP (2006) Mater Sci Forum 503–504:805
17. Islamgaliev R, Kulyasova O, Mingler B, Schafler E, Korb G, Karnthaler HP, Zehetbauer M (2006) Proc Ultrafine Grained Materials IV, TMS 06 Annual Conference, San Antonio, March 2006, eds. Zhu YT, Langdon TG, Horita Z, Zehetbauer M, Semiatin SL, Lowe TC p. 407
18. Kulyasova OB, Islamgaliev RK, Valiev RZ (2005) Phys Met Metallogr 100:277 (in Russian)
19. Massalski B (1990) ''Binary Alloy Phase Diagrams–Second Edition'' (ASM International, Materials Park, Ohio)
20. Chinh NQ, Szommer P, Horita Z, Langdon TG (2006) Adv Mater 18:34
21. Schafler E, Steiner G, Korznikova E, Kerber M, Zehetbauer M (2005) Mater Sci Eng A 410:169
22. Bassani P, Gariboldi E, Tuissi A (2005) J Therm Anal Calor 80:739
23. Korznikova E, Schafler E, Steiner G, Zehetbauer MJ (2006) Proc Ultrafine Grained Materials IV, TMS 06 Annual Conference, San Antonio, March 2006, eds. Zhu YT, Langdon TG, Horita Z, Zehetbauer M, Semiatin SL, Lowe TC, p. 97